Mode observations and confinement characterization during configuration scans in Wendelstein 7-X

T. Andreeva[1]*, M. Hirsch[1], G. Wurden[2], A. Alonso[3], C. D. Beidler[1], M. Beurskens[1], S. Bozhenkov[1], R. Brakel[1], C. Brandt[1], K. J. Brunner[1], R. Burhenn[1], V. Bykov[1], A. Dinklage[1], G. Fuchert[1], J. Geiger[1], M. Grahl[1], O. Grulke[1], U. Höfel[1], M. Jakubowski[1], G. Kocsis[4], T. Klinger[1], J. Knauer[1], A. Krämer-Flecken[5], A. Langenberg[1], S. Lazerson[6], U. Neuner[1], C. Nührenberg[1], N. Pablant[6], K. Rahbarnia[1], J. Schilling[1], J. C. Schmitt[7], H. Thomsen[1], E. Trier[8], T. Windisch[1], J. Zhu[1], S. Zoletnik[4], and the W7-X Team

[1] *Max-Planck-Institute for Plasma Physics, Wendelsteinstr. 1, 17491 Greifswald, Germany*

[2] *Los Alamos National Laboratory, Los Alamos, NM, 87545, USA*

[3] *Laboratorio Nacional de Fusión, CIEMAT, Av. Complutense 40, 28040 Madrid, Spain*

[4] *Wigner RCP RMI, Budapest, Hungary*

[5] *Institute for Climate and Energy Research – Plasma Physics, Forschungszentrum Jülich, 52425 Jülich, Germany*

[6] *Princeton Plasma Physics Laboratory, Princeton NJ, 08543, USA*

[7] *Auburn University, Auburn, AL, U.S.A*

[8] *Max-Planck-Institute for Plasma Physics, Boltzmannstraße 2, 85748 Garching, Germany*

Introduction

Wendelstein 7-X (W7-X) is a modular advanced stellarator (Greifswald, Germany), which successfully finished its test-divertor-unit experimental campaign in October 2018. Besides establishing divertor operation, this campaign was devoted to the verification of the optimization principles of the machine [1]. In addition, configuration scans were performed between several reference magnetic configurations with the aim to analyse confinement and performance changes by the gradual successive variation of the rotational transform. Experiments, done at the predecessor stellarator Wendelstein 7-AS, showed, that in low-to-medium density experiments small changes in iota near rational iota values could lead to significant variation of confinement (20% difference in performance) [2].

Magnetic configuration space and technical realization of scans

The magnet system of W7-X consists of 50 non-planar (NPC) and 20 planar (PC) superconducting coils, which are arranged in five identical modules and allow realization of a large variety of magnetic configurations [3]. Configurational scans reported in this paper were conducted between high iota and standard magnetic configurations. Reference standard and high-iota configurations have, respectively, five and four islands outside the last closed magnetic surface (LCMS) and are characterized by $\iota/2\pi$=5/5 and 5/4, correspondingly. The advantage of the high-iota magnetic configuration is that it has an almost negligible value of the bootstrap current at low densities, and, hence, one can more easily differentiate between various possible impacts on confinement properties.

High-iota magnetic configuration is characterized by negative identical coil currents of approximately -10 kA per winding (in each out of 36 windings) in each PC, having identical non-planar coil currents of approximately 14 kA per winding (in each of 108 windings) in each NPC. Nominal standard magnetic configuration is characterized by identical coil currents of approximately 13 kA per winding in all NPC, having zero currents in PCs. In order to compensate for the change of iota due to the coil deformations under electromagnetic loads, the nominal planar coil currents had to be reduced by 250 A in all investigated configurations. The intermediate (between high-iota and standard) configurations were achieved by the gradual change of the planar coil currents. PC currents in all scanned configurations as well as Poincaré plots of three configurations in the scan, demonstrating different island location, are shown in Fig.1.

discharge	configuration	PC cur. [A]
20180927.09	FTM001+252	-10040
20180927.15	FQM001+252	-7290
20180927.16	FOM003+252	-5040
20180927.17	FNM+252	-4790
20180927.18	FNM001+252	-4540
20180927.19	FNM002+252	-4290
20180927.20	FMM+252	-4040
20180927.21	FMM001+252	-3790
20180927.22	FMM002+252	-3540
20180927.27	FMM003+252	-3290
20180927.29	FLM+252	-3040
20180927.30	EJM+252	-1040
20180927.33	EJM004+252	-250

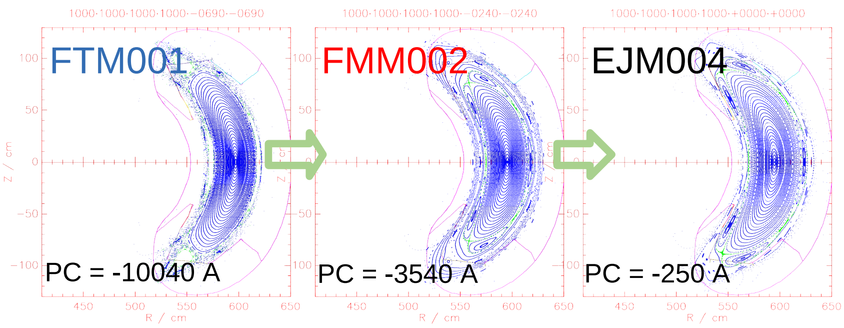

Fig.1 Poincaré plots for the scan between high iota (FTM001) and standard (EJM004) configurations.

Input discharge parameters (ECRH power and density) were kept identical in all configuration scans. The typical discharge of 4 seconds is shown in Fig. 2.

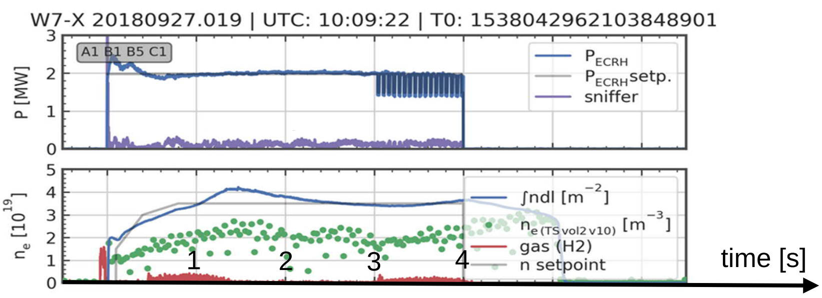

Fig.2 Typical discharge during iota scans.

Experimental observations

Fig. 3 demonstrates the measured diamagnetic energy and corresponding confinement time in conducted configuration scans. Both continuously increased starting high-iota magnetic configuration up to the approximately intermediate FLM configuration, and afterwards gradually decreased towards the standard magnetic configuration. Fig. 4 shows the corresponding values of the rotational transform and of the plasma volume. Rotational transform was obtained by means of the V3FIT code (equilibrium reconstruction code utilizes several diagnostic signals and geometric divertor information, in a non-linear optimization algorithm with singular-value decomposition to rapidly calculate the equilibrium state of 3-D magnetically confined plasmas) [4]. Plasma volume was calculated by a Fourier representation of the cylindrical co-ordinates R, ϕ and Z, describing the LCMS obtained by field-line tracing.

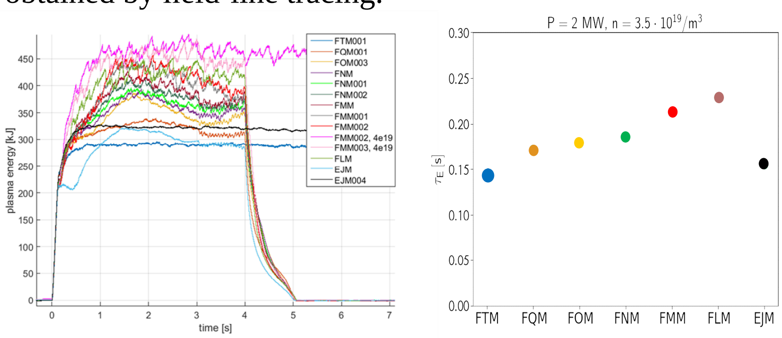

Fig.3 Diamagnetic energy and confinement time in configuration scans.

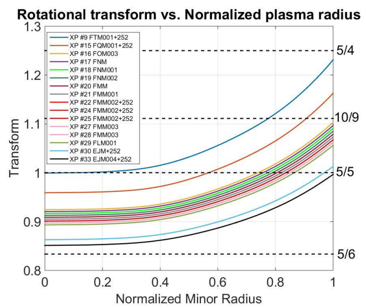

configuration	volume (m³)
FTM001+252	25.2
FQM001+252	30.6
FOM003+252	30.9
FNM+252	31.1
FNM001+252	31.2
FNM002+252	31.3
FMM+252	30.9
FMM001+252	31.6
FMM002+252	31.5
FMM003+252	31.4
FLM+252	32
EJM+252	27.6
EJM004+252	30.2

Fig.4 V3FIT reconstruction of the rotational transform and corresponding volume of all scanned configurations.

At the same time, various diagnostics (e.g., segmented Rogowski coils, soft X-ray tomography system, correlation reflectometry, video diagnostics) demonstrated a mode activity, increasing up to the intermediate FLM configuration and further decreasing towards the standard case. Experiments to relate this mode activity to the size of internal islands (almost all scanned intermediate configurations had a chain of 5/5 islands within the LCMS) revealed that the mode activity grows with the increase of the island size, and decreases with the island size reduction. Nevertheless, the diamagnetic energy stayed in these experiments at the same level independent of the island size. Fig. 5 shows mode activity, detected by the correlation reflectometry in configurations with a fine iota step, and change of the mode activity intensity in discharges with different island size, demonstrated by video diagnostics.

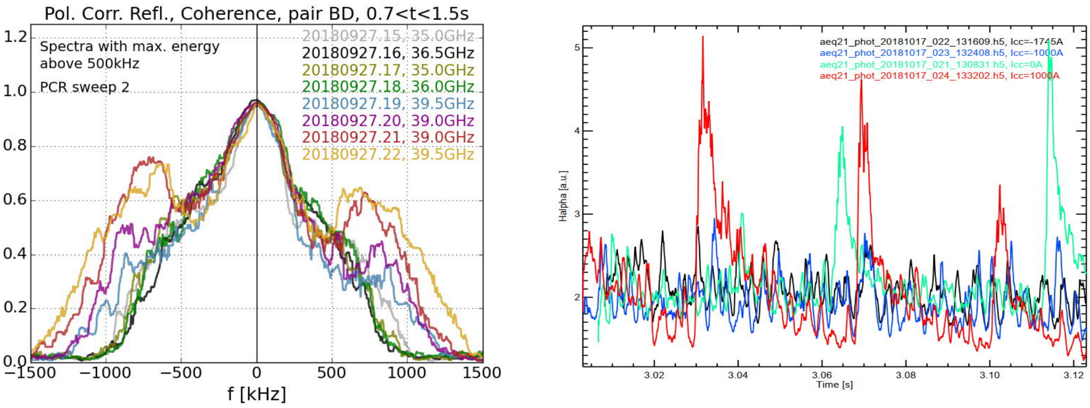

Fig.5 Mode activity detected by the correlation reflectometry system (left) and change of the mode activity in discharges with different island size (right).

Summary

In configuration scans, conducted between standard and high-iota magnetic configurations, rotational transform variation revealed an increase of the diamagnetic energy and confinement time in several intermediate limiter configurations. These observations were accompanied by the appearance of mode activity, shown by various diagnostics. The mode activity correlates with the size of the internal islands and becomes more intense with the island enlargement, decreasing with the reduction of the island size. The change of the island size seems to have no effect on the diamagnetic energy in the discharges with identical densities and heating power.

This work has been carried out within the framework of the EUROfusion Consortium and has received funding from the Euratom research and training programme 2014-2018 and 2019-2020 under grant agreement number 633053. The views and opinions expressed herein do not necessarily reflect those of the European Commission

References

1. G. Grieger, et al., “Modular stellarator reactors and plans for Wendelstein 7–X”, Fusion Technol. 21 (1992) 1767-1778.

2. M. Hirsch, et al., “Major results from the stellarator Wendelstein 7-AS”, Plasma Phys. Control. Fusion 50 (2008) 053001 (204pp).

3. T. Andreeva, et al., “Characteristics of main configurations of Wendelstein 7-X”, Problems of Atomic Science and Technology, Series: Plasma Physics, Vol. 4 (2002) 45-47.

4. J.D. Hanson, D.T. Anderson, M. Cianciosa, et al., “Non-axisymmetric equilibrium reconstruction for stellarators, reversed field pinches and tokamaks”, Nucl. Fusion 53 083016 (2013).